Sensing and Bio-Sensing Research 5 (2015) 55–61

Contents lists available at ScienceDirect

Sensing and Bio-Sensing Research

journal homepage: www.elsevier.com/locate/sbsr

Rapid light transmittance measurements in paper-based microfluidic devices

Christina Swanson [a,1,*], Stephen Lee [b,1], A.J. Aranyosi [b], Ben Tien [a], Carol Chan [a], Michelle Wong [a], Jared Lowe [b], Sidhartha Jain [a], Roozbeh Ghaffari [b,*]

[a] Diagnostics for All, Inc., 840 Memorial Drive, Cambridge, MA 02139, USA
[b] MC10, Inc., 9 Camp Street, Cambridge, MA 02140, USA

ARTICLE INFO

Article history:
Received 13 April 2015
Revised 17 June 2015
Accepted 6 July 2015

Keywords:
Paper microfluidics
Colorimetric
Light transmission
Alanine aminotransferase
Enzymatic reactions
Continuous monitoring

ABSTRACT

We developed methodology and built a portable reader to assess light transmittance in paper-based microfluidic devices in a highly sensitive, user-friendly and field-appropriate manner. By sandwiching the paper assay between micro-light-emitting diodes and micro-photodetectors, the reader quantifies light transmittance through the paper independent of ambient light conditions. To demonstrate the utility of the reader, we created a single-use paper-based microfluidic assay for measurement of alanine aminotransferase, an indicator of liver health in blood. The paper assay and reader system accurately differentiated alanine aminotransferase levels across the human reference range and demonstrated significant differences at clinically relevant cutoff values. Results were provided within 10 min and were automatically generated without complex image analysis. Performance of this point-of-care diagnostic rivals the accuracy of lab-based spectrometer tests at a fraction of the cost, while matching the timeliness of low-cost portable assays, which have historically shown lower accuracy. This combination of features allows flexible deployment of low cost and quantitative diagnostics to resource-poor settings.

1. Introduction

Microfluidic paper-based analytical devices (μ-PADs) with colorimetric readouts have gained popularity as low-cost, rapid diagnostic tools [9,13]. Scientists have developed μ-PADs for a wide range of functions, from rapid point-of-care measurement of liver enzyme levels to routine evaluation of heavy metal contamination in reservoir water [17,20]. While these devices can provide highly accurate and sensitive diagnostic information, they are often highly multiplexed with complicated geometries and multi-color readout [5,9,10,16,20]. Further, color development may depend on time, temperature and humidity.

The increasing complexity of colorimetric μ-PADs, which makes visual interpretation of results challenging, necessitates the development of novel methods for data acquisition. Towards enhancing the objectivity and quantitative value of results, researchers have employed light reflectance measurements using line scan readers, charge-coupled device (CCD)-based readers, smart phone cameras and variations thereof [8,11,12,14,20,21]. However, the nature of light reflectance measurements, which obtain information from only the light absorbing particles in the top 10–20 μm of the paper, may artificially limit μ-PAD sensitivity [22].

With paper thicknesses commonly ranging from 50 to 400 μm, light transmission measurements offer enhanced accuracy and sensitivity by interrogating the cumulative density of light absorbing particles throughout the thickness of the paper [7]. Further, sensitivity may be tuned by layering sheets of paper to create different thicknesses [6]. However, user-friendly methods to quantify colorimetric results in μ-PADs using light transmission have not been demonstrated due to several technical challenges concerning the paper substrate and sample matrix. Foremost, dry white paper, depending on its thickness and density, strongly reflects light resulting in less than 25% of incident light being transmitted through the paper [1]. This limits the possible range of light intensity differences that can be directly caused by concentration changes in the μ-PADs. To enhance the percent of incident light that is transmitted through paper, the paper may be wetted. Previous groups have saturated the μ-PAD with vegetable oil, however, this may be cumbersome in a point-of-care setting [6]. Further, because light transmission directly depends on the dampness of the paper, the μ-PAD must be kept uniformly wet over the time period of the assay [3]. This is difficult because the small

* Corresponding authors.
E-mail addresses: cswanson@dfa.org (C. Swanson), rghaffari@mc10inc.com (R. Ghaffari).
[1] These authors contributed equally.

http://dx.doi.org/10.1016/j.sbsr.2015.07.005
2214-1804/

sample volumes quickly evaporate from the large surface area of the paper and because paper as a substrate is variable. Across a single sheet of paper, thickness and fiber density may vary up to 5%, altering light transmission and wetting [1]. In addition to the intrinsic properties of paper, the hematological traits of biological samples may cause difference in their light absorption capacity and viscosity. These variations can cause disparities in the degree of wetting, the capillary flow rate, and ultimately the light transmission through the μ-PAD.

To overcome these technical challenges and enable light transmission measurement of colorimetric μ-PADs in a user-friendly manner, we developed novel methodology in three areas. First, we sealed μ-PADs to limit evaporation at the test areas and stabilize light transmission properties over the time period of the assay. Second, we designed and built a highly sensitive reader to measure light transmittance from multiplex assays. We demonstrate a portable reader in which a paper-based assay is sandwiched between micro-LEDs and micro-photodetectors. The reader works independent of different light conditions, has a miniaturized and multiplexed format, automatically generates transmittance values that do not require image analysis and is made of affordable parts. Third, we developed procedures for reader calibration and data collection. These procedures effectively normalize differences in light transmittance arising from paper and sample variability.

This paper details the engineering of our transmittance-based reader system and presents evidence of its function through rapid assessment of liver function using quantification of alanine aminotransferase (ALT) concentrations in human serum. Section 2 describes the manufacturing of the reader-compatible μ-PAD, the engineering theory, components and function of the reader, and the alignment and calibration techniques employed for measurements. Section 3 uses the μ-PAD and reader for quantification of ALT in human serum samples and compares the sensitivity of the system to a scanner-based method. Sections 4 and 5 discuss results and provide conclusions and future directions.

2. Materials and methods

2.1. Paper microfluidics

While μ-PADs have previously been developed to measure ALT levels in plasma and blood, they contained multiple layers and were optimized for visual interpretation and semi-quantitative analysis of results [18]. To create an ALT assay that is compatible with our transmittance-based reader, we developed a device consisting of a single-layer of paper (Fig. 1a). In our new layout, each device consisted of a single sample port area and four arms, each comprising a channel leading to a circular storage zone and a circular read zone. We incorporated separate storage and read zones because prior work indicated that spatially separating the enzymes and substrates in two different areas enhanced the stability of the device. The storage zones and read zones were both 3 mm in diameter to allow adequate deposition of reagents and adequately encircle the 1.5 mm × 1.5 mm LEDs/PDs (Fig. 1b). To manufacture the devices, we created the device pattern in Adobe Illustrator CS3 and printed the pattern on Whatman No. 1 chromatography paper (GE Healthcare) using a ColorQube 8870 printer (Xerox) [4]. Each sheet of assays was passed through an EconRed I oven (Vastex International) at 204 °C to melt the wax into the paper and create the hydrophobic barriers.

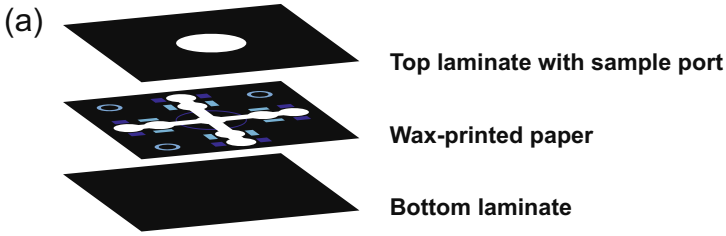

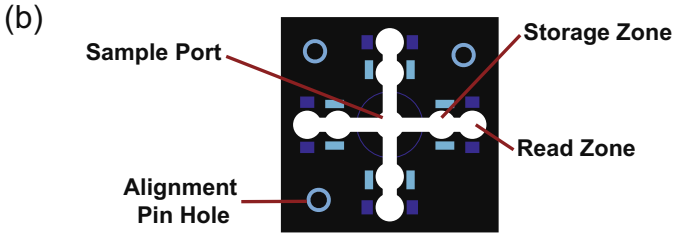

(c)

L-alanine + α-ketoglutarate $\xrightarrow{\text{ALT}}$ pyruvate + glutamate **(1)**

pyruvate + phosphate + O_2 + H_2O $\xrightarrow[\text{TPP, } Mg^{+2}]{\text{PO}}$ acetylphosphate + CO_2 + H_2O_2 **(2)**

H_2O_2 + 4-AAP + DAOS $\xrightarrow{\text{HRP}}$ blue dye complex **(3)**

Fig. 1. Paper assay design. (a) The assay consisted of a single paper layer enclosed by top and bottom laminate layers. (b) The wax-printed paper layer consisted of a sample port and four individual arms. Each arm had two circular areas, a storage zone where reagents were dried on the paper and a read zone where color developed. After serum was applied to the sample port, capillary forces in the paper rapidly distributed the serum into the four individual arms of the assay filling up the storage zone and read zone consecutively. (c) Equations of chemical reactions (1–3) used to form a blue dye complex at a rate that corresponds with the ALT concentration in the applied serum. Alanine transaminase (ALT), pyruvate oxidase (PO), thiamine diphosphate (TPP), 4-aminoantipyrine (4-AAP) and N-ethyl-N-(2-hydroxy-3-sylfopropyl)-3,5-dimethoxyalanine (DAOS). (For interpretation of the references to color in this figure legend, the reader is referred to the web version of this article.)

To determine the concentration of ALT in serum, we modified a previously published sequence of chemical reactions to increase reaction speed and produce a deep blue color that strongly absorbs red light (Fig. 1c, Eqs. 1–3) [18]. In these reactions, ALT catalyzes the formation of pyruvate and glutamate from L-alanine (Acros Organics, New Jersey USA) and alpha-ketoglutarate (Sigma–Aldrich, St. Louis, MO, USA). The pyruvate reacts to form hydrogen peroxide in the presence of pyruvate oxidase (Sekisui, Japan). Horseradish peroxidase (Sigma–Aldrich, St. Louis, MO, USA), using hydrogen peroxide, then oxidizes 4-aminoantypyrine and N-ethyl-N-(2-hydroxy-3-sylfopropyl)-3,5-dimethoxyalanine (DAOS) (both from Sigma–Aldrich, St. Louis, MO, USA) to form a blue dye complex [18].

Following wax printing and sealing of the paper, we applied color forming reagents to the storage zones and read zones. In the storage zone, we spotted 0.50 μL of Reagent 1 consisting of 1 M alanine, 30 mM alpha-ketoglutarate and 200 mM phosphate buffer. In the read zone, we spotted 0.50 μL of Reagent 2 consisting of 0.9 mM NaH_2PO_4, 12.5 U/L pyruvate oxidase, 0.9 mM thiamine pyrophosphate, 9 mM $MgCl_2$, 14.4 mM 4-aminoantypyrine, 6.4 mM DAOS, 11.25 U/L horse radish peroxidase, 45 mg/mL polyethylene glycol (M.W. 35,000), 10 mg/mL BSA and 200 mM phosphate buffer. All devices were dried at room temperature for five minutes.

To minimize fluid loss from evaporation, we sealed each assay with self-adhesive plastic sheets (Fellowes). The plastic sheets were chosen because they allow airflow while impeding fluid movement. We completely enclosed the backside of each assay with the plastic laminating sheets, pressing the devices into the laminate utilizing a bench top laminator (Apache AL13P) to ensure good contact. For the front of the assay, we designed a top laminate that completely covered the storage and read zones, while allowing easy sample addition. Front laminate sheets were cut into square sections with 7.5 mm diameter holes using a knife plotter (CraftROBO pro). For each device, we applied laminate directly on top of the center of a dried paper assay and pressed to ensure good contact. For alignment with the pins in the reader, we punched three 1.5 mm holes in each device at specific, pre-marked locations. Assays were stored at room temperature in a desiccator box until use.

2.2. Optoelectronics

Quantitation of the assay was made possible through integration with the BioStampDx™ optoelectronic platform developed at MC10 Inc (Fig. 2a). The paper device was sandwiched between two parts of an electrical circuit designed to interrogate light transmission through the paper. An optoelectronic circuit illuminated the test locations with light-emitting diodes (LEDs) having a center wavelength $\lambda = 642$ nm (Fig. 2b and c). Light was transmitted through the chromatography paper substrate and detected by a photodiode (PD) with peak sensitivity at $\lambda = 620$ nm (Fig. 2b). These wavelengths were chosen to maximize the absorption of light by the blue dye complex while minimizing the absorption

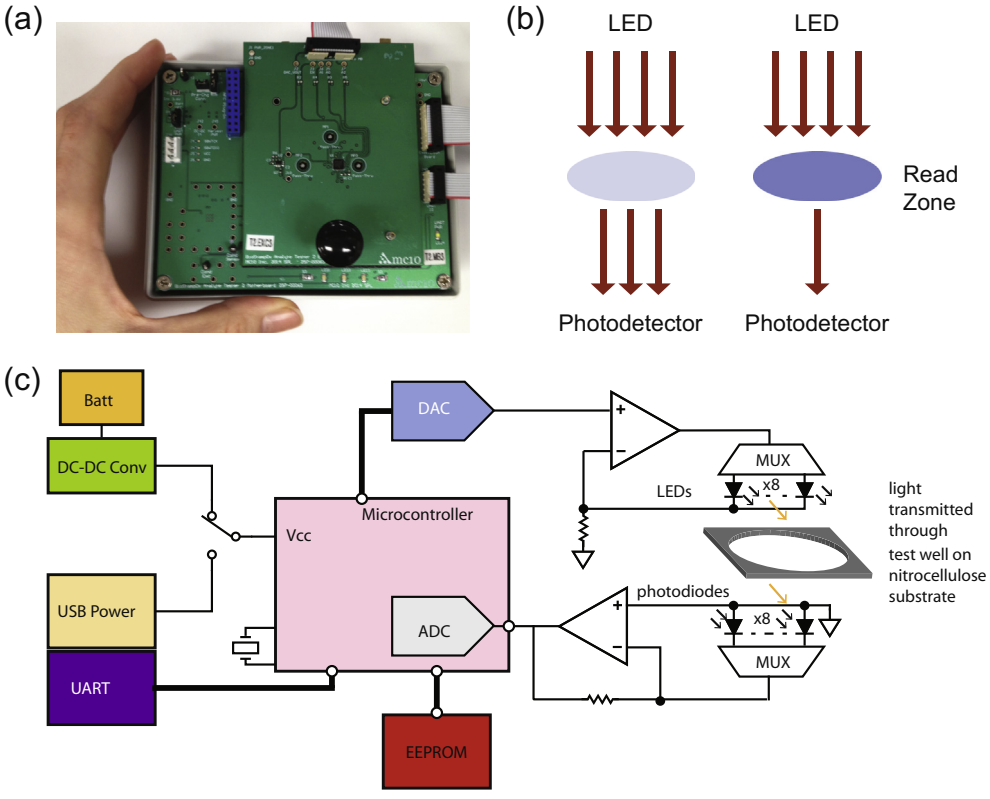

Fig. 2. Design of handheld portable reader. (a) The reader consists of photodetectors that have been placed on a rigid printed circuit board. Attached through a hinge is a lid that contains the LEDs. The hinge allows for easy placement of the paper assay between the LEDs and PDs and provides repeatable alignment of the LEDs and PDs. Between the paper assay and electronics, two plastic spacers have been added to align the paper to the sensors and control the separation of the LEDs and PDs. The entire system is connected through a USB port to a laptop where software collects and analyzes data from the system. (b) An LED/PD pair surrounds the read zone on each arm of the assay. When there are low ALT levels and little blue dye complex forms, most of the light from the red LEDs passes through the read zone and is detected by the PD. When there are high ALT levels and a lot of blue dye complex forms, more of the light from the red LEDs is blocked by the read zone and less light is detected by the PD. (c) Diagram of internal electronics. LED intensity can be incremented in 1024 steps. Each photodetector and LED pair is multiplexed – sharing the same transimpedance amp and LED driver reducing channel to channel variability. The microcontroller steps the DAC over a pre-set time increment, ensuring that the circuitry has settled before each measurement and maintaining consistency across repeated measurements. (For interpretation of the references to color in this figure legend, the reader is referred to the web version of this article.)

by possible blood contaminants such as hemoglobin which absorbs light strongly below 600 nm [3,23]. Each test and control site was measured by a respective excitation LED and photodiode pair. The intensity of excitation was controlled by a voltage controlled current source, which in turn was adjusted by a 10-bit digital-to-analog converter. A transimpedance amplifier circuit converted the current from the photodiode to a voltage digitized bya 10-bit analog to digital converter (Fig. 2c).

The diagnostic was operated by a microcontroller (MSP430, Texas Instruments) with firmware written in C using a state-machine design. The state machine cycled through channels, activating the appropriate LED and PD for each. At each location the state machine cycled the LED through a range of drive currents while measuring the corresponding sense current at the PD. The state machine was programmed to provide the amplifiers and analog to digital converter enough settling time for accurate and reliable measurements. Each measurement was stored in non-volatile memory and/or transferred to a computer in real time. Between clocked data samples, the microcontroller was put to sleep to conserve power. The system had two operating modes: it could be powered by a universal serial bus (USB) connection to a desktop or laptop computer and controlled using an accompanying desktop application, or powered from a battery while operating independently with data stored in non-volatile memory for later retrieval.

Channel to channel variation was reduced by multiplexing the excitation amplifier amongst all LED channels; likewise the photodiode amplifier was multiplexed between measurement channels. This left the majority of channel variation to LED and photodiode tolerance. The remaining error was mitigated through software calibration based on control measurements as described below.

Both the voltage controlled current source and transimpedance amplifier exploited feedback topologies that reduced the number of components and cost. Furthermore they were designed to operate on a low supply rail so that this system can be deployed in the field using a laptop USB connection or inexpensive batteries. Tests showed that varying the supply voltage by 10% produced less than a 1% variation in measurement results. The device is configured to be able to measure battery voltage to ensure it is within spec. Respective multiplexers at the voltage controlled current source and at the transimpedance amplifier ensured an independent measurement on each channel. Rail to rail, low power, auto-zeroed amplifiers were selected to reduce errors due to offset and $1/f$ noise while maintaining low power consumption.

2.3. Alignment, calibration and error sources

The microchannels and read zones of the paper assay were aligned using alignment pillars and holes punched through the assay. To reduce the error from alignment issues, we designed 3 mm diameter read zones to readily accommodate the 1.5 mm^2 photodetector windows. Thus, the assay can be up to 0.75 mm out of alignment on all sides and results should remain similar. Moreover, intentionally shifting the assay by 0.5 mm produced no significant change in test results.

At each measurement location the photodiode output was measured for a range of LED currents. The relation between LED current and photodiode output was characterized by a nonlinear equation. The best fit of this equation to the data was computed using a weighted least-squares approach, and the gain of this fit was taken as a measure of light transmittance through the assay. For each assay, the gain was first measured when the assay was dry, immediately following sample application. At this time, the serum had not flowed into the read zone. This calibration corrected for variations in properties of the optoelectronics, assay dimensions and alignment, paper fiber density, dust, etc. All subsequent measurements were normalized to this dry gain. Following the dry calibration, light transmittance through each read zone was measured every 15 s for 15 min. Wetting of the read zone by serum increased the transparency of the assay, increasing the gain. Following this wetting, the amount of blue dye complex formed in each individual read zone reduced optical transmission according to the Beer–Lambert law [2], leading to a reduction in gain over time. The reaction rate was then calculated as the slope of this reduction, mitigating the effects of varying flow rates and light transmission properties of the serum.

3. Results

Because dry paper transmits light poorly, it was critical to measure light transmission at the read zone when the paper was fully wetted. This increased the possible range of light intensity differences that could be directly caused by changes in the buildup of blue-dye complex at the read zone. Further, the read zone had to be kept uniformly wet over the time period of the assay because light transmission directly depends on the dampness of the paper. Previously, Ellerbee et al. measured light transmission in colorimetric paper by placing the paper assays in plastic sleeves and saturating them in vegetable oil [6]. Because this method is unwieldy for the field and may introduce errors, we designed a μ-PAD that was pre-sealed on the front and back with plastic laminate. To enhance user-friendliness, a small sample port was left open on the front side for easy sample addition (Fig. 1a).

To explore the effects of evaporation on our μ-PAD, we added 12.5 μL of human serum (Valley Biomedical, VA, USA) to the sample port of assays and tracked their change in weight for 15 min – the normal duration of our enzymatic assay. In testing conditions of 21 °C and 15% relative humidity, our assays lost an average of 0.3 μL of fluid each minute (Fig. 3a). As this is a significant (36%) decrease in fluid volume over the time period of the assay, we examined if this evaporation from the open sample port area affected light transmission at the read zones. For each assay, we added 12.5 μL of serum and measured the change in light transmittance at the read zone for 15 min. In contrast to the evaporation

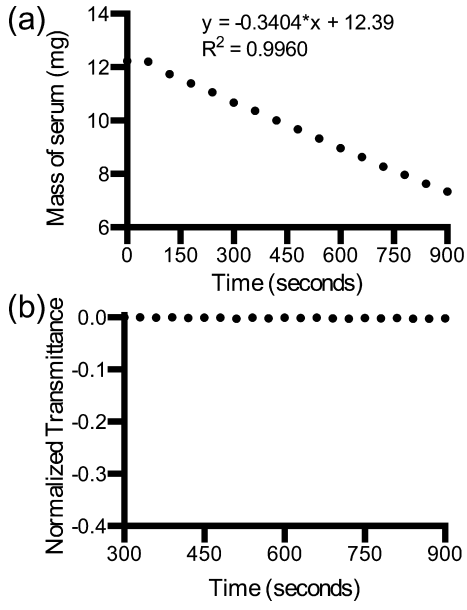

Fig. 3. Light transmission stability over time. (a) Fluid volume lost from the device over a 900 s (15 min) period. (b) Normalized light transmittance at read zones. The normalized light transmittance values were calculated as the gain at the time of measurement minus the gain at 300 s. Bars indicating standard errors are smaller than data point markers.

measurements, the light transmittance at the read zone changed less than 1% over the 15-min period (Fig. 3b). Together, these measurements indicate that sealing the read zone area with laminate prevented evaporation from this specific area and maintained its light transmitting properties.

To demonstrate the function of our portable transmittance reader, we collected data from our ALT assay over a wide range of ALT concentrations in human serum. For each concentration, we tracked the light transmission through four read zones in two assays. To run each ALT assay, we placed the assay in the reader and added 12.5 μL of human serum spiked with ALT (Leebio Solutions, MO, USA). We closed the lid of the tester, performed an initial calibration on the dry assay to correct for variation in LED strength and assay alignment, and then took light transmittance measurements every 15 s for 15 min.

The measured gain for each channel changed in a predictable manner over the course of the 15-min read time. Initially, the gain was normalized to 1 for all read zones in the dry state. As capillary forces pulled the serum into the four channels and to the read zones, the read zones became completely wet and their light transmittance increased substantially. This was seen as a large increase in the gain as compared to the dry state (Fig. 4). When ALT was present, blue dye complex formed in the read zone and increased in concentration over time. The build up of the blue dye complex absorbed red light, reducing the amount of light transmitted and reducing the gain over time (Fig. 4). For this comparison of wet to dry read zones over time, the gain was normalized to 1 for all read zones in the dry state, Gain(t)/Gain(0 s).

To determine the rate of dye accumulation for each ALT concentration, the gain values measured from 300 to 900 s were normalized to the 300 s value, Gain(t)/Gain(300 s). Normalization to the 300 s value was chosen because the read zone was fully wetted by 300 s, but no significant color had developed. The average of these gain values over time was plotted and demonstrated strong differentiation between the different ALT concentrations (Fig. 5a). The reaction rate was calculated as the slope of each set of measurements between 300 and 600 s and plotted versus the ALT concentration. The reaction rate changed linearly with ALT concentration ($y = -0.002421 * x + 0.03822$, $R^2 = 0.9104$). To determine if the change in reaction rate for each ALT concentration was able to differentiate clinically elevated ALT levels, we performed a student's t-test to compare each concentration to 25 U/L. An upper limit of normal (ULN) of 25 U/L was chosen as a cutoff value because resent studies have found that the ULN for ALT depends on age, gender and BMI and may range from 17 to 66 U/L depending on the sampling population [15]. All values above and including 50 U/L were significantly different than 25 U/L with p-values less than or equal to 0.002 (Fig. 5b). In addition, the reaction rates for serum with 6 U/L also differed significantly from those with 25 U/L demonstrating a p-value less than 0.0001 (Fig. 5b).

In addition to collecting light transmittance data for each ALT assay, we also scanned each assay with a flatbed scanner 16 min after serum addition. Representative scans of each ALT concentration demonstrate that it was visually difficult to differentiate low concentrations of ALT (Fig. 6a). To imitate data collected by a reflectance reader, we quantified the average pixel intensity in the read zones using ImageJ software and plotted these values for each ALT concentration [19]. Similar to the light transmission reader, the average pixel intensity changed linearly over the range of ALT concentrations ($y = 0.1747 * x + 191.8$, $R^2 = 0.9242$). To determine if the change in average pixel intensity for each ALT concentration was significantly different, we performed a student's t-test to compare the pixel intensity at each concentration to that at 25 U/L. Although values above 50 U/L were significantly different from 25 U/L, the value for 6 U/L was not (Fig. 6b).

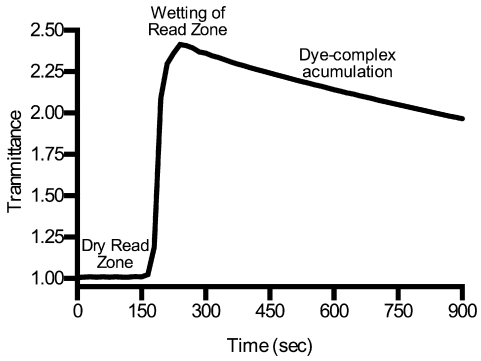

Fig. 4. Change in light transmittance over duration of ALT assay. The light transmittance of all channels in the dry state is normalized to a gain of 1. As serum flows from the sample port to the read zone, it completely wets the read zone leading to a large increase in light transmittance of the paper, which is visualized as a large increase in the gain. If ALT is present, blue dye complex forms at the read zone, increasing over time. The blue dye complex absorbs light, reducing the amount of light transmitted through the paper. This is seen as a reduction in the gain over time.

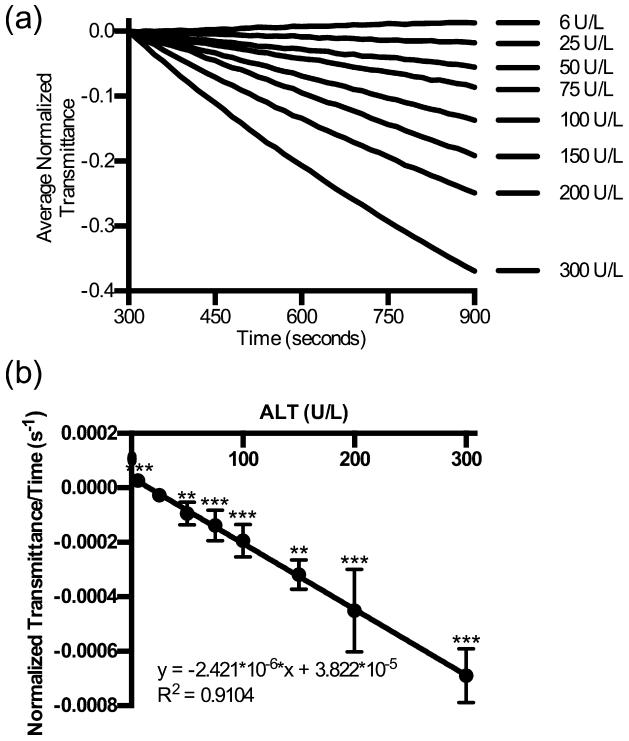

Fig. 5. Measurement of ALT concentration with portable transmittance reader. Serum with different concentrations of ALT was added to assays and the light transmittance at each read zone recorded every 15 s for 15 min. (a) Normalized light transmittance values were calculated as the gain at the time of measurement minus the gain at 300 s. All values at a given concentration and time point were averaged. (b) Reaction rates were calculated as the slope of the normalized light transmittance versus time for each read zone between 300 and 600 s. Average and standard errors of the slope value at different ALT concentrations is plotted. $n = \geqslant 4$. **Indicates a p-value of <0.01 and ***indicates a p-value <0.001.

4. Discussion

The diagnostic system presented here enables rapid, point-of-care light transmittance measurements from colorimetric μ-PADs as demonstrated by measurement of ALT concentration in small volumes of serum. Sealed μ-PADs limited evaporation from the read areas enabling stable light transmittance over the time

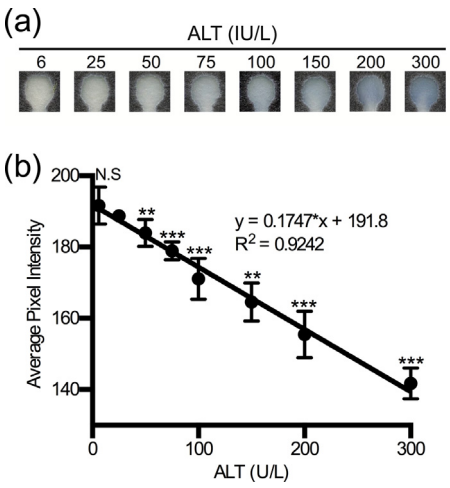

Fig. 6. Measurement of ALT concentration with scanner. Individual ALT assays were scanned at 16 min following analysis in portable transmission reader. (a) Representative images of read zones for each ALT concentration. (b) The pixel intensity of the read zones was analyzed in image J. The average pixel intensities and standard errors are plotted for each ALT concentration. $n = \geqslant 4$. Bars indicate standard errors. N.S. indicates non-significant. **Indicates a p-value of <0.01 and ***indicates a p-value <0.001.

period of the assay. Color formation from different concentrations of ALT built up over time, allowing quantitation within 10 min with the reader and within 16 min with the scanner. The diagnostic can measure ALT concentration in a sample from 6 to 300 U/L, which is the normal human range. Further, the diagnostic showed similar differentiation of low concentrations of ALT as scanning and image analysis.

This diagnostic system has several advantages over existing solutions. It only requires a small amount of serum, so blood samples can be taken from a finger stick rather than a venous draw. The paper-based portion of the diagnostic is small, low-cost and disposable, allowing a health care worker to take a large number of assays to remote locations. Unlike previous transmission-based systems, this system is easier to use because pre-wetting with vegetable oil is unnecessary [6]. Instead, the read zones of the paper assay are sealed with plastic film to minimize evaporation and the paper remains wet throughout the duration of measurement period.

The reader is portable and robust. Unlike many other paper-based point-of-care diagnostics, our approach is highly miniaturized and quantitative, allowing sensitive detection of small concentrations of ALT with high precision. The reader is self-contained with its own processor, allowing it to be used in environments where no power is available. It can be operated by battery or through a USB connection to a laptop or other portable device. It is self-calibrating, eliminating the need for external standards or comparison to central lab facilities. Finally, it can be re-used indefinitely, but is also inexpensive enough to be easily replaced as needed.

Slope based measurements enhance the accuracy of the data for two reasons. First, many data points are collected over the duration of the experiment. The slope is then calculated from all of these data points, making final measurements more resilient to individual read errors and outliers. Second, by measuring the slope instead of the endpoint, slight differences in the thickness of the paper at different points do not significantly affect the measurement.

Alternate approaches for quantifying colorimetric μ-PADs assays include the use of scanners or mobile phone cameras. Line scan readers, such as the ESEQuant Lateral Flow System (Qiagen, CA, USA), successfully collect data from LFAs. However, they are incompatible with the complex geometries often found in μ-PADs. Charge-coupled device (CCD)-based readers capture data quickly over a wide area, but are often expensive and require skilled image analysis [8]. Smart phone cameras and corresponding applications capture assay images and compare assay color development to an accompanying color chart [20]. While these offer a simple, cost-effective solution for point-of-care assays, results are vulnerable to changes in environmental lighting, photo angle and depth, and differences in the make/model of the phone. Similarly, cell phone-attached, enclosed LFA readers, which attach to the back of a cell phone and use internal LEDs for illumination, continue to use a cell phone's camera making them dependent on the make/model of the phone [14]. Lastly, portable light reflectance readers, which collect data on signal intensity by measuring the light reflected from the surface of an assay, lack sensitivity because they are not able to sample the density of absorbers throughout the thickness of the paper [11,12,21]. These approaches measure reflected light, which is dominated by the optical properties of the surface. Consequently, they may not accurately sample the density of absorbers in the assay.

The limitations of this diagnostics platform include initial usage of human serum rather than whole blood, controlling the reader with a computer and low throughput. Although the current diagnostic requires serum or plasma rather than whole blood, plasma may be readily separated by incorporation of a commercial plasma separation membrane. Furthermore, while measurements presented here used a USB connection to a computer for power and data transfer, a 1.5 V battery can power the system. Moreover, the microcontroller has sufficient computational power to quantify the results and store them in non-volatile memory for later retrieval by any of a variety of methods. The current system has relatively low throughput, measuring a single assay in ~10 min. However, the low cost and small size of the paper assays and optoelectronics make it possible to deploy an array of diagnostics in resource-limited environments.

5. Conclusions

We have demonstrated a user-friendly diagnostics system that enables automatic light transmittance measurements from colorimetric μ-PADs. We utilize this system to measure ALT concentration in serum. Sealing the assays allowed us to minimize evaporation at the read zones. Because we performed continuous measurements to calculate a reaction rate, we reduce the inherent noise caused by variations in the paper substrate, sample and flow speeds. Together, these advancements not only freed the user from data interpretation, but also decreased the read time to 10 min which is a significant improvement over the 20–30 min required for endpoint ALT assays [17].

Overall, this diagnostic system is highly flexible and shows future potential for collection of data from colorimetric assays. In a miniaturized format, dozens of reactions could be placed on a 2 cm^2 paper assay and produce different colors on the paper. For each of those reactions, a specific LED/PD pair could be chosen to optimize light transmittance measurements. The thickness of the paper, concentration of the reagents, and design of the electronics could be tailored to target a specific concentration range. Because of the inherent affordability of paper and the minimal volume of enzymes and substrates used in the assay, overall cost is estimated at less than $0.10 per device. In large-scale production, the readout electronics are expected to cost less than 20 US dollars. Together, this could allow for a disposable, rapid, low-cost device that evaluates numerous blood analytes simultaneously and can be deployed in far reaches of the world that lack infrastructure.

Acknowledgements

The authors thank Brian Murphy, Barry Ives, Jared Lowe, Suzy Hong, and Kirsten Seagers for technical support and discussions. The authors thank the Bill & Melinda Gates Foundation, Grant #OPP1086152, for their generous support.

References

[1] A. Adams, M. Fahrenwald, L. Do, Measurement and modeling of light transmission through turbid media, J. Ark. Acad. Sci. 61 (2007) 1–3.
[2] A. Beer, Bestimmung der absorption des rothen lichts in farbigen flussigkeiten. Annalen der Physik und Chemie. 86 (1852).
[3] M. Bond, C. Elguea, J.S. Yan, M. Pawlowski, J. Williams, A. Wahed, M. Oden, T.S. Tkaczyk, R. Richards-Kortum, Chromatography paper as a low-cost medium for accurate spectrophotometric assessment of blood hemoglobin concentration, Lab Chip 13 (2013) 2381.
[4] E. Carrilho, A.W. Martinez, G.M. Whitesides, Understanding wax printing: a simple micropatterning process for paper-based microfluidics, Anal. Chem. 81 (2009) 7091–7095.
[5] W. Dungchai, O. Chailapakul, C.S. Henry, Analytica Chimica Acta, Anal. Chim. Acta 674 (2010) 227–233.
[6] A.K. Ellerbee, S.T. Phillips, A.C. Siegel, K.A. Mirica, A.W. Martinez, P. Striehl, N. Jain, M. Prentiss, G.M. Whitesides, Quantifying colorimetric assays in paper-based microfluidic devices by measuring the transmission of light through paper, Anal. Chem. 81 (2009) 8447–8452.
[7] E. Evans, E.F.M. Gabriel, W.K.T. Coltro, C.D. Garcia, Rational selection of substrates to improve color intensity and uniformity on microfluidic paper-based analytical devices, Analyst 139 (2014) 2127.
[8] C. Gui, K. Wang, C. Li, X. Dai, D. Cui, A CCD-based reader combined with CdS quantum dot-labeled lateral flow strips for ultrasensitive quantitative detection of CagA, Nanoscale Res. Lett. 9 (2014) 1–8.
[9] J. Hu, S. Wang, L. Wang, F. Li, B. Pingguan-Murphy, T.J. Lu, F. Xu, Biosensors and bioelectronics, Biosens. Bioelectron. 54 (2014) 585–597.
[10] J.C. Jokerst, J.A. Adkins, B. Bisha, M.M. Mentele, L.D. Goodridge, C.S. Henry, Development of a paper-based analytical device for colorimetric detection of select foodborne pathogens, Anal. Chem. 84 (2012) 2900–2907.
[11] D.-S. Lee, B.G. Jeon, C. Ihm, J.-K. Park, M.Y. Jung, A simple and smart telemedicine device for developing regions: a pocket-sized colorimetric reader, Lab Chip 11 (2010) 120–126.
[12] B. Li, L. Fu, W. Zhang, W. Feng, L. Chen, Portable paper-based device for quantitative colorimetric assays relying on light reflectance principle, Electrophoresis 35 (2014) 1152–1159.
[13] A.W. Martinez, S.T. Phillips, M.J. Butte, G.M. Whitesides, Patterned paper as a platform for inexpensive, low-volume, portable bioassays, Angew. Chem. Int. Ed. 46 (2007) 1318–1320.
[14] O. Mudanyali, S. Dimitrov, U. Sikora, S. Padmanabhan, I. Navruz, A. Ozcan, Integrated rapid-diagnostic-test reader platform on a cellphone, Lab Chip 12 (2012) 2678.
[15] L. Pacifico, F. Ferraro, E. Bonci, C. Anania, S. Romaggioli, C. Chiesa, Clinica Chimica Acta, Clin. Chim. Acta 422 (2013) 29–39.
[16] N.R. Pollock, D. Colby, J.P. Rolland, A point-of-care paper-based fingerstick transaminase test: toward low-cost "lab-on-a-chip" technology for the developing world, Clin. Gastroenterol. Hepatol. 11 (2013) 478–482.
[17] N.R. Pollock, S. McGray, D.J. Colby, F. Noubary, H. Nguyen, T.A. Nguyen, S. Khormaee, S. Jain, K. Hawkins, S. Kumar, J.P. Rolland, P.D. Beattie, N.V. Chau, V.M. Quang, C. Barfield, K. Tietje, M. Steele, B.H. Weigl, Field evaluation of a prototype paper-based point-of-care fingerstick transaminase test, PLoS ONE 8 (2013) e75616.
[18] N.R. Pollock, J.P. Rolland, S. Kumar, P.D. Beattie, S. Jain, F. Noubary, V.L. Wong, R.A. Pohlmann, U.S. Ryan, G.M. Whitesides, A paper-based multiplexed transaminase test for low-cost, point-of-care liver function testing, Sci. Trans. Med. 4 (2012) 1–20.
[19] C.A. Schneider, W.S. Rasband, K.W. Eliceiri, NIH Image to ImageJ: 25 years of image analysis, Nat. Methods 9 (2012) 671–675.
[20] H. Wang, Y.-J. Li, J.-F. Wei, J.-R. Xu, Y.-H. Wang, G.-X. Zheng, Paper-based three-dimensional microfluidic device for monitoring of heavy metals with a camera cell phone, Anal. Bioanal. Chem. 406 (2014) 2799–2807.
[21] M. Yamaguchi, S. Kambe, T. Eto, M. Yamakoshi, T. Kouzuma, N. Suzuki, Point of care testing system via enzymatic method for the rapid, efficient assay of glycated albumin, Biosens. Bioelectron. 21 (2005) 426–432.
[22] A.K. Yetisen, M.S. Akram, C.R. Lowe, Paper-based microfluidic point-of-care diagnostic devices, Lab Chip 13 (2013) 2210.
[23] W.G. Zijlstra, A. Buursma, W.P. Meeuwsen-van der Roest, Absorption spectra of human fetal and adult oxyhemoglobin, de-oxyhemoglobin, carboxyhemoglobin, and methemoglobin, Clin. Chem. 37 (1991) 1633–1638.